The heme oxygenase-1 metalloporphyrin inhibitor stannsoporfin enhances the bactericidal activity of a novel regimen for multidrug-resistant tuberculosis in a murine model

Jennie Ruelas Castillo[1], Pranita Neupane[1], Styliani Karanika[1], Stefanie Krug[1,⊥], Darla Quijada[1], Andrew Garcia[1], Samuel Ayeh[1], Diego L Costa[3, 4], Alan Sher[5], Nader Fotouhi[6], Natalya Serbina[6], Petros C Karakousis[1,2,7*]

[1] Center for Tuberculosis Research, Department of Medicine, Johns Hopkins University School of Medicine, Baltimore, MD, USA

[2] Department of International Health, Johns Hopkins Bloomberg School of Public Health, Baltimore, MD, USA

[3]Departmento de Bioquímica e Imunologia, Faculdade de Medicina de Ribeirão Preto, Universidade de São Paulo, Ribeirão Preto, Brazil

[4]Departamento de Imunologia, Instituto de Ciências Biomédicas, Universidade de São Paulo, São Paulo, Brazil

[5]Immunobiology Section, Laboratory of Parasitic Diseases, National Institute of Allergy and Infectious Diseases, National Institutes of Health, Bethesda, MD, USA

[6] TB Alliance, New York, NY, USA

[7] Department of Molecular Microbiology and Immunology, Johns Hopkins Bloomberg School of Public Health, Baltimore, MD, USA

[⊥] Department of Microbiology, University of Washington School of Medicine, Seattle, WA 98195, USA

[*] Correspondence:
Center for Tuberculosis Research
CRB-2

1550 Orleans St., Room 110

Baltimore, MD 21287

petros@jhmi.edu

Abstract:

Multidrug-resistant (MDR) *Mycobacterium tuberculosis* (Mtb) poses significant challenges to global tuberculosis (TB) control. Host-directed therapies (HDT) offer a novel approach for TB treatment by enhancing immune-mediated clearance of Mtb. Prior preclinical studies found that inhibition of heme oxygenase-1 (HO-1), an enzyme involved in heme metabolism, with tin-protoporphyrin IX (SnPP) significantly reduced mouse lung bacillary burden alone and when co-administered with the first-line antitubercular regimen. Here we evaluated the adjunctive HDT activity of a novel HO-1 inhibitor, stannsoporfin (SnMP), in combination with a novel MDR-TB regimen containing human-equivalent doses comprising a next-generation diarylquinoline, TBAJ-876 (S), pretomanid (Pa), and a new oxazolidinone, TBI-223 (O) (collectively, SPaO) in Mtb-infected BALB/c mice. After 4 weeks of treatment, SPaO + SnMP 5 mg/kg reduced mean lung bacillary burden by an additional 0.69 $\log_{10}$ (P=0.0145) relative to SPaO alone. As early as two weeks post-treatment initiation, SnMP adjunctive therapy differentially altered the expression of pro-inflammatory cytokine genes, and CD38, a marker of M1 macrophages. Next, we evaluated the sterilizing potential of SnMP adjunctive therapy in a BALB/c relapse model. After six weeks of treatment, SPaO + SnMP 10 mg/kg reduced lung bacterial burdens to 0.71 ± 0.23 $\log_{10}$ CFU, a 0.78 log-fold greater decrease in lung CFU compared to SpaO alone. Although adjunctive SnMP did not reduce microbiological relapse rates after 6 weeks of treatment, mice receiving this regimen exhibited the lowest lung CFU upon relapse. SnMP is a promising HDT candidate requiring further study in combination with regimens for drug-resistant TB.

Keywords: *Mycobacterium tuberculosis*, Host-directed therapies, Heme-oxygenase 1, chemotherapy, drug resistance

Introduction:

Mycobacterium tuberculosis (Mtb) is the causative agent of tuberculosis (TB), a deadly disease that claims millions of lives yearly. The emergence of multidrug-resistant TB (MDR TB), which is resistant to at least two of the most potent first-line drugs, rifampin, and isoniazid, is a significant challenge to global health [1], [2]. The World Health Organization estimated that in 2021, there were 465,000 new cases of MDR TB worldwide, and only 60% of these cases were treated successfully [1]. MDR-TB treatment is lengthy, complex, expensive, and requires the use of second-line drugs that are less effective and more toxic, highlighting the urgent need for novel therapeutics [3], [4]. Given the global burden of MDR TB, host-directed therapies (HDT) targeted at boosting the immune system have the potential to contribute to tuberculosis control to prevent further cross-resistance with current antibiotics [5], [6].

Heme oxygenase-1 (HO-1) is an enzyme involved in the degradation of heme into biliverdin, carbon monoxide (CO), and iron [7]–[10]. HO-1 is a known biomarker for active TB in humans [11]. HO-1 also plays a crucial role in the survival of Mtb inside the host by suppressing immune responses and promoting bacterial growth [12]. Several studies have shown that Mtb infection induces HO-1 expression in macrophages [8], [13], leading to the generation of CO, which has immunomodulatory properties and can suppress the production of pro-inflammatory cytokines, such as TNF-α, IL-1β, and IL-6 [14], [15]. Additionally, the production of CO can inhibit the activity of T cells and natural killer cells, which are essential components of the host immune response against Mtb [16]. HO-1 induction can drive macrophage polarization towards an anti-

inflammatory, M2 phenotype, which is associated with reduced microbicidal activity [17], [18] and increased persistence of Mtb in the host [19].

Several studies have highlighted the potential utility of HO-1 inhibitors as HDT for TB. Costa *et al.* showed previously that pharmacological inhibition of HO-1 with the metalloporphyrin tin protoporphyrin (SnPP) during the chronic phase of infection in the C57BL/6 murine model of TB reduced the lung bacillary burden alone and when co-administered with human-equivalent doses of the standard regimen for drug-susceptible TB [20]. HO-1 inhibition promoted the differentiation of $CD4^+$ T cells into interferon gamma (IFNγ)-producing Th1 cells. Additionally, SnPP enhanced IFN-γ-dependent, nitric oxide synthase 2 (NOS2)-induced nitric oxide production by macrophages, resulting in enhanced control of bacterial growth [21]. Another compound in this class, the HO-1 inhibitor stannsoporfin (SnMP), has been in clinical development as a therapy for hyperbilirubinemia in neonates [22]. SnMP has been shown to induce the activation, proliferation, and maturation of naïve $CD4^+$ and $CD8^+$ T cells via interactions with $CD14^+$ monocytes in *vitro* [23].

In the current study, we compared the adjunctive bactericidal activity of SnPP and SnMP when co-administered with a novel MDR-TB regimen containing TBAJ-876 (S), pretomanid (Pa), and TBI-223 (O)) (collectively, SPaO) or the first-line drug regimen (rifampin (R), isoniazid (H), and pyrazinamide (Z); collectively, RHZ) against chronic TB infection in BALB/c mice. In addition, we tested the ability of SnMP to shorten the duration of curative treatment in a murine model of microbiological relapse.

Results:

In chronically infected BALB/c mice, adjunctive therapy with SnMP increases the bactericidal activity of SPaO

We investigated SnPP and SnMP as adjunctive HDT agents in BALB/c mice infected with Mtb (Fig 1A). Each compound was given alone or co-administered with human-equivalent doses of the first-line regimen RHZ for a total of 6 weeks or the enhanced-potency MDR regimen SPaO for a total of four weeks. In a previous study [20], SnPP was dosed at 5 mg/kg, but was increased to 10 mg/kg to have similar drug exposure as SnMP. Plasma pharmacokinetics profiles were determined for SnPP and SnMP up to 8 hours post administration. SnPP 10 mg/kg and SnMP 5 mg/kg achieved similar 24-hour drug exposure in plasmas (Fig S1), supporting the use of these dosages were selected for the primary study. After two weeks of treatment (Fig 1C, Table1), monotherapy with SnPP 10 mg/kg or SnMP 5 mg/kg reduced the mean lung bacillary burden by 0.88 $\log_{10}$ and 0.67 $\log_{10}$ colony-forming units (CFU), respectively, relative to the vehicle control. At the same time point, SnPP or SnMP adjunctive therapy showed no additive effect when co-administered with SPaO. However, after four weeks of treatment (Fig 1D), SPaO + SnMP 5 mg/kg reduced the mean lung bacillary burden to 2.49 ± 0.12 $\log_{10}$ CFU, representing an additional 0.69 $\log_{10}$ CFU reduction compared to SPaO alone ($p = 0.014$). In contrast, SnMP did not enhance the bactericidal activity of RHZ ($p=0.13$), even after six weeks of treatment (Fig 1E). Conversely, treatment with SnPP alone reduced bacterial burden by a mean of 1.1 $\log_{10}$ CFU ($p=0.001$) relative to vehicle.

HO-1 inhibition does not exacerbate lung inflammation and regulates pro-inflammatory immune responses.

The chronic stages of TB disease are characterized by severe lung inflammation, which results in long-term lung dysfunction in one-quarter of cases despite microbiological cure [24], [25]. HO-1$^{-/-}$ knock-out mice develop a progressive inflammatory state [13], [26], and splenocytes isolated from these mice respond to LPS stimulation by producing inflammatory cytokines [4], [13]. Chronic treatment with SnPP in wild-type mice can induce tubulointerstitial inflammation and fibrosis [27], while SnMP induces the expression of pro-inflammatory cytokines in human peripheral blood mononuclear cells [28]. Robust expression of pro-inflammatory cytokines can exacerbate lung inflammation but, when controlled, can offer antimycobacterial protection to the host [29]. To determine whether HO-1 inhibition modulates TB-associated lung pathology, we analyzed the lung weight to body weight (lung/body) ratio of Mtb-infected mice treated with SnPP or SnMP alone or as adjunctive HDT with RHZ or SPaO as a gross indicator of lung inflammation. Antitubercular treatment with RHZ or SPaO significantly reduced ($p < 0.0001$) the mean lung/body ratio relative to vehicle at all time points (Fig 2A-C). SnMP or SnPP monotherapy also significantly reduced lung/body weight ratio after 2 and 6 weeks relative to vehicle (Fig 2A,C), while there was a nonsignificant decrease after 4 weeks of treatment (Fig 2B). These results suggest that lung inflammation generally correlated with lung CFU burden in each of the treatment groups (Fig 1). Next, lung histopathology was evaluated by hematoxylin and eosin stain after 4 weeks of treatment to determine if SnMP had any impact on cellular infiltration in the lungs (Fig 2D). We observed no major differences in lung histopathology between the treatment groups, regardless of HO-1 inhibition. These data suggest that HO-1 inhibition does not negatively impact the resolution of lung inflammation with TB treatment.

In order to investigate the adjunctive contribution of SnMP to the bactericidal activity of SPaO observed at 4 weeks of treatment (Table 1), we used RT-qPCR to evaluate the expression of pro-inflammatory cytokine genes and macrophage markers in lung homogenates at week 2, prior to a significant difference in lung bacillary burden between the various groups. NOS2 expression in macrophages is upregulated in response to Mtb infection and IFNγ activation is required for successful bacterial load reduction following pharmacological inhibition of HO-1 [21]. IFN-γ and tumor necrosis factor-alpha (TNF-α) are important pro-inflammatory T-cell macrophage-activating cytokines [30], [31]. SnMP monotherapy had lower expression of NOS2 ($p < 0.05$, Fig 3A), IFN-γ ($p < 0.05$, Fig 3B) and TNF-α ($p < 0.01$, Fig 3C) relative to vehicle, while SPaO alone or with SnMP had even lower expression of NOS2 ($p < 0.001$) and IFN-γ ($p < 0.01$). The decrease in cytokine production is likely a host response to the decrease in bacterial buden at this timpoints from these therapies. TNF-α expression was comparable in SnMP, SPaO, and SPaO + SnMP-treated mice. Next, we looked for expression changes in the mouse macrophage markers CD38 and early growth response protein 2 (EGR2), a transcriptional regulator/M1 marker and a negative T-cell regulator/M2 marker, respectively [32], [33]. SnMP monotherapy, but not adjunctive therapy with SPaO, resulted in significantly higher expression of CD38 ($p < 0.0001$) compared to any other treatment group (Fig 3D). In contrast, EGR2 expression (Fig 3E) did not differ significantly between groups. Overall, these data are consistent with reduced expression of pro-inflammatory cytokine genes as a result of reduced mean lung CFU in the treatment groups (Table 1). However, SnMP treatment also appears to induce the expression of CD38, polarizing lung macrophages to an M1 phenotype, which is more effective in killing intracellular Mtb.

SnMP adjunctive therapy enhances the bactericidal efficacy of SPaO after 6 weeks of treatment without impacting relapse rates but reduces bacterial burdens in relapsed mice

Next, we evaluated the adjunctive sterilizing activity of SnMP at different dosages in combination with SPaO. We selected treatment durations expected to yield > 50% relapse rates for the backbone regimen based on the prior literature [34]. The mice were treated for a total of 5 or 6 weeks, at which time the treatment was discontinued, and microbiological relapse was assessed 3 months later (Fig 4A). Adjunctive therapy with SnMP 5 mg/kg (SnMP5) did not significantly alter lung bacillary burdens relative to the SPaO regimen at the time points assessed. However, after 6 weeks of treatment, SPaO + SnMP 10 mg/kg (SnMP10) reduced mean lung bacterial burdens to 0.71 ± 0.23 $\log_{10}$ CFU, representing an additional 0.78 $\log_{10}$ CFU reduction ($p < 0.001$) when compared to SPaO alone (Fig 4B, Table 1). Alike the primary animal study, SnMP5 or SnMP10 therapy with SpaO significantly ($p < 0.0001$) reduced the lung/body ratio relative to the W0 UNT group and interestingly mice in the relapse groups sustained the same weights throughtout the three months wait period (Fig S2). All mice had microbiological relapse following 5 weeks of treatment with SpaO or SpaO + SnMP10 (Fig 4C); however, mice treated with SpaO + SnMP10 had significantly lower bacterial burdens than SpaO-treated mice (1.5 $\pm$ 1.1 vs. >3 $\log_{10}$ CFU, respectively; $p = 0.03$). Following 6 weeks of treatment, the proportion of relapsing animals was equivalent in the groups receiving SPaO and SpaO + SnMP10 (66%); however, the mean lung bacillary burden was 1.9 $\pm$ 1.0 $\log_{10}$ and 1.4 $\pm$ 1.1 $\log_{10}$ $\log_{10}$ CFU in these groups, respectively (Fig 4D).

Discussion:

Inhibition of HO-1 has been proposed as a potential HDT strategy associated with reduced Mtb growth in vitro [35] and in vivo [20], [21]. Our study investigated the adjunctive bactericidal activity of a clinical-stage HO-1 inhibitor, SnMP, in a mouse model of chronic TB, as well as its adjunctive sterilizing activity when combined with a MDR-TB regimen in a murine model of microbiological relapse. We found that adjunctive therapy of SnMP enhanced the bactericidal activity of the SPaO regimen, but not that of the RHZ regimen, without exacerbating lung inflammation. Although adjunctive therapy with SnMP10 continued to enhance the bactericidal activity of SPaO after 6 weeks, it did not alter relapse rates compared to SPaO alone.

In contrast with prior work [20], we did not find additive bactericidal activity of SnPP with RHZ in Mtb-infected mice. These discrepant findings may be explained by differences in experimental design, bacterial burden at the start of treatment or due to different mouse models used in each study. In the study by Costa *et al.*, C57BL/6 mice were used, while our study used BALB/c mice. Relative to BALC/c mice, C57BL/6 mice are able to more effectively limit the replication of Mtb through the development of T-cell-mediated immunity [36], [37]. Interestingly, this discrepancy was observed only when SnPP was given as adjunctive therapy, as we found that SnPP monotherapy reduced lung bacillary burden, as was reported previously [20]. These findings higlight the challenges associated with preclinical studies of HDT for TB, as the host-directed activity of these agents may be model-specific.

Our studies showed that SnMP administered alone regulated the expression of the genes encoding NOS2, IFN-γ, and TNF-α in the lungs. Scharn *et al*. have shown previously that SnPP

reduced the secretion of proinflammatory cytokines, including TNF-α, in Mtb-infected U937 cells [37], [24]. Notably, CD38 expression was upregulated in Mtb-infected mouse lungs following treatment with SnMP alone. Although CD38 is necessary for immune cell activation and is expressed by many immune cell types [38], it appears to be a specific marker for M1 macrophage phenotypes in murine models [33]. In humans and in mice, M1 macrophages play an essential role in propagating a host protective response against Mtb (reviewed in Ahmad et al, 2022) [39], [40]. Collectively, these results highlight an immunoregulatory role for the HO-1 inhibitor SnMP during Mtb infection. Additional studies are needed to further characterize the molecular mechanisms by which SnMP promotes Mtb clearance by the host.

Due to the results of the time course study and based on published data where the SPaO regimen, at different dosages, had eliminated relapse in lung bacterial burden by week 7 [34], the relapse time points of 5 and 6 weeks were selected to evaluate adjunct therapy of SnMP. Although we had high numbers of relapsed animals by week 6, mice receiving the SPaO + SnMP5 or SnMP10 regimen had the lowest mean bacterial burden upon relapse. While SPaO + SnMP10 had the highest number of relapse animals with countable CFU, SPaO + SnMP5 retained the lowest CFU among animals with countable CFUs for the W6 + 3M relapse group. Higher doses of SnMP need to be tested to firmly validate which dosage has the strongest effect on eliminating bacterial burden in the relapse setting.

Consistent with prior preclinical studies [20], [21], [35], we have found that HO-1 inhibition is a promising HDT strategy for TB. We show for the first time that the novel HO-1 inhibitor, SnMP, enhances the bactericidal activity of the novel MDR-TB regimen SPaO in mice and modulates

the expression of several pro-inflammatory cytokine and macrophage marker genes, which have been implicated in the control of Mtb replication in vivo. Although the proportion of relapsing animals was equivalent between mice receiving SPaO with or without SnMP, the latter group had a lower lung bacillary burden at the time of relapse. Overall, this study advances our understanding of HO-1 inhibitors as potential adjunctive HDT agents for TB, but further research is needed to determine the potential utility of targeting this pathway against drug-susceptible and drug-resistant TB.

Materials and Methods:

Pharmacokinetic analyses:

Single-dose PK studies were conducted by BioDuro Inc. (Beijing, China). SnMP and SnPP were formulated in sodium phosphate buffer (pH 7.4 – 7.8) and administered by intraperitoneal route to 9–11-week-old female BALB/c mice. Three mice were used per each time point with 8 time points for each dose group. Blood was collected on 0.25, 0.5, 1, 2-, 4-, 8-, and 24-hours post-administration and levels of compounds in plasma were quantified by liquid chromatography-tandem mass spectrometry using AB Sciex API 4000 LC/MS/MS instrumentation. The following PK parameters were calculated from plasma drug concentrations: t1/2, tmax, Cmax, AUClast, AUCInf. All parameters were determined using were determined by noncompartmental analysis using WinNonLin software 8.0.

Bacteria and growth conditions:

Wild-type Mtb H37Rv was grown in Middlebrook 7H9 broth (Difco, Sparks, MD) supplemented with 10% oleic acid-albumin-dextrose- catalase (OADC, Difco), 0.2% glycerol, and 0.05% Tween-80 at 37°C in a roller bottle.

M. tuberculosis infection of mice:

Female BALB/c (8-10-week-old, Jackson Laboratory) were aerosol-infected using a Glas-Col Inhalation Exposure System (Terre Haute, IN) calibrated to deliver ~100 bacilli of wild-type Mtb H37Rv to the lungs of mice.

Antibiotic and HDT treatments:

In the bactericidal activity studies, the mice received one of the following regimens beginning 28 days after aerosol infection: 1) Vehicle (negative control); 2) protoporphyrin IX (SnPP) 10 mg/kg; 3) stannsoporfin (SnMP) 5 mg/kg; 4) rifampin (R) 10 mg/kg, isoniazid (H) 25 mg/kg, pyrazinamide (P) 150 mg/kg (collectively, RHZ); 5) TBAJ 876 (S) 6.25 mg/kg, pretomanid (Pa) 30 mg/kg and TBI-223 (O) 45 mg/kg (collectively, SPaO); 6) R 10 mg/kg, H 25 mg/kg, P 150 mg/kg, SnPP 10 mg/kg; 7) R 10 mg/kg, H 25 mg/kg, P 150 mg/kg, SnMP 5 mg/kg; 8) S 6.25 mg/kg, Pa 30 mg/kg, O 45 mg/kg, SnPP 10 mg/kg; 9) S 6.25 mg/kg, Pa 30 mg/kg, O 45 mg/kg, SnMP 5 mg/kg . The HO-1 inhibitors were given once daily by intraperitoneal injection. PK analysis of the HO-1 inhibitors were conducted at 5 mg/kg and 10 mg/kg to test which dosages achieved similar plasma concentrations. There results also confirmed that the dosages achieved human-equivalent doses [41]. The other drugs were given orally by esophageal cannulation once daily, except for Pa and O, which were given twice daily separated by at least 4 hours. For the RHZ regimen, R was given first, and two hours later, H and Z were administered.

The vehicle administered was either cyclodextrin micelle (CM-2) formulation containing 10% hydroxypropyl-β-cyclodextrin (Sigma) and 10% lecithin (ICN Pharmaceuticals Inc., Aurora, OH) to mock Pa, 0.5% methylcellulose to mock O or 20% hydroxypropyl- b-cyclodextrin solution acidified with 1.5% 1N HCl to mock S. They were administered via gavage to the mice concurrent to the treatments containing the active compounds.

In the relapse model studies, the mice received one of the following regimens beginning 28 days after aerosol infection: 1) Vehicle (negative control); 2) S 6.25 mg/kg, Pa 30 mg/kg, O 45 mg/kg; 3) S 6.25 mg/kg, Pa 30 mg/kg, O 45 mg/kg, SnMP 5 mg/kg; or 4) S 6.25 mg/kg, Pa 30 mg/kg, O 45 mg/kg, SnMP 10mg/kg. The discrepancies in numbers of animals between relapse groups is due to unexpected mortality from excessive gavage volume when the drugs were prepared separately at the start of therapy. Beginning in week 2, 2X concentrations of Pa and O were made and at time of administration PaO were mixed at equal volumes to make a single gavage volume of 0.2 mL which the mice tolerated well.

For both studies (except for the relapse time points, for which both lobes of the lung were homogenized and plated), the right lung and 3/5 of the left lung of each mouse were homogenized using glass homogenizers, and serial tenfold dilutions of lung homogenates in PBS were plated on 7H11 selective agar (BD) at the indicated time points. Plates were incubated at 37°C and CFU were counted 4 weeks later. For the animals in the relapse groups, the whole lung was used for CFU. All procedures were performed according to protocols approved by the Johns Hopkins University Institutional Animal Care and Use Committee.

Histology:

At the time of harvest, the left lung medial apex to base was sectioned and fixed with 4% paraformaldehyde (PFA). After a 24-hour incubation in 4% PFA, the lung section was transferred to PBS and sent in for processing. The lung section was sectioned to 4 μm and stained with hematoxylin and eosin (H&E). The histology slides were imaged with the Nikon Fluorescence Dissection w/SLR at the JHU SoM MicFac center.

Cytokine or cell marker gene expression:

A section of the left lower lobe (~ 1/5 of the left lung) was flash-frozen in liquid nitrogen at the time of harvest and later lysed in TRIzol using a hard tissue homogenizing kit (CK28-R, Percellys). Total RNA was extracted using the miRNeasy minikit (217004, Qiagen). RT-qPCR sequences for each primer pair used in these studies were ordered from IDT and are listed in the supplementary material Table 2. Two-step RT-qPCR was performed on a StepOnePlus real-time PCR system (ThermoFisher Scientific) using the high-capacity RNA-to-cDNA kit (4387406, ThermoFisher Scientific) followed by Power SYBR green PCR master mix (436877, Applied Biosystems).

Statistics:

The differences between groups were assessed using one-way ANOVA followed by multiple comparison tests. The Prism software (GraphPad, San Diego, CA, USA) version 9 was utilized for this analysis. Results were considered statistically significant when the p-value was less than 0.05.

Supplemental material:

Figure S1: Plasma pharmacokinetic parameters for SnPP and SnMP in mice

Figure S2: Mice ratio of whole lung weight(g)/body weight(g) after 6 weeks of treatment and at the relapse timepoint

Table 2: RT-qPCR sequences for each primer pair

Author Contributions:

PN, SKa, NS, and PCK conceived and designed the time course study. NS provided data and the description for the pharmokinetic study. PN, SKa, SA administered the therapies; PN, SKa, SKr, performed animal haversting, tissue sectioning and weight collection, plated the homogenates of the infected lungs, collected CFU and analysed CFU data for the time course study. JRC performed data analysis for the lung/body weights. JRC imaged the histology slides. JRC extracted RNA from lung tissue. JRC and DQ performed RTqPCR experiements, and performed data analysis. JRC, PN, Ska, NS, and PCK conceived and designed the relapse study. JRC, and PN administered the therapies for the relapse study. JRC, PN, and Ska performed animal haversting, tissue sectioning and weight collection; PN, JRC, and AG plated the homogenates of the infected lungs; JRC, PN performed CFU data collection and analysis for the relapse study. JRC, and PCK drafted the manuscript. JRC, PN, Ska, SKr, DQ, AG, SA, DLC, AS, NF, NS, and PCK interpreted the data and edited the manuscript. All authors edited and approved the final manuscript.

Acknowledgments: These studies were supported by NIAID/NIH grant K24AI143447 and a grant from the TB Alliance to PCK. AS is supported by the intramural research program of the

NIAID. We thank the Oncology Tissue Services (SKCCC) at JHU supported by the P30 CA006973 grant. We also thank the Johns Hopkins University School of Medicine Microscope Facility for training and the use of their microscope.

Ethics statement: The animal study was reviewed and approved by Johns Hopkins University Institutional Animal Care and Use Committee.

References:

[1] World Health Organization, "Global Tuberculosis Report 2022," 2022. Geneva: World Health Organization; 2022.

[2] K. J. Seung, S. Keshavjee, and M. L. Rich, "Multidrug-resistant tuberculosis and extensively drug-resistant tuberculosis," *Cold Spring Harb Perspect Med*, vol. 5, no. 9, Sep. 2015, doi: 10.1101/cshperspect.a017863.

[3] E. Pontali *et al.*, "Regimens to treat multidrug-resistant tuberculosis: Past, present and future perspectives," *European Respiratory Review*, vol. 28, no. 152. European Respiratory Society, 2019. doi: 10.1183/16000617.0035-2019.

[4] C. Lange, D. Chesov, J. Heyckendorf, C. C. Leung, Z. Udwadia, and K. Dheda, "Drug-resistant tuberculosis: An update on disease burden, diagnosis and treatment," *Respirology*, vol. 23, no. 7, pp. 656–673, Jul. 2018, doi: 10.1111/resp.13304.

[5] D. J. Frank *et al.*, "Remembering the host in tuberculosis drug development," in *Journal of Infectious Diseases*, Oxford University Press, May 2019, pp. 1518–1524. doi: 10.1093/infdis/jiy712.

[6] G. Kilinç, A. Saris, T. H. M. Ottenhoff, and M. C. Haks, "Host-directed therapy to combat mycobacterial infections*," *Immunological Reviews*, vol. 301, no. 1. John Wiley and Sons Inc, pp. 62–83, May 01, 2021. doi: 10.1111/imr.12951.

[7] R. Tenhunen, H. S. Marver, and R. Schmid, "The enzymatic conversion of heme to bilirubin by microsomal heme oxygenase.," *Proc Natl Acad Sci U S A*, vol. 61, no. 2, pp. 748–55, Oct. 1968, doi: 10.1073/pnas.61.2.748.

[8] S. W. Ryter and A. M. K. Choi, "Heme oxygenase-1/carbon monoxide: From metabolism to molecular therapy," *American Journal of Respiratory Cell and Molecular Biology*, vol. 41, no. 3. pp. 251–260, Sep. 01, 2009. doi: 10.1165/rcmb.2009-0170TR.

[9] M. D. Maines, "THE HEME OXYGENASE SYSTEM: A Regulator of Second Messenger Gases," 1997. [Online]. Available: www.annualreviews.org

[10] S. W. Ryter and R. M. Tyrrell, "The heme synthesis and degradation pathways: role in oxidant sensitivity. Heme oxygenase has both pro- and antioxidant properties.," *Free Radic Biol Med*, vol. 28, no. 2, pp. 289–309, Jan. 2000, doi: 10.1016/s0891-5849(99)00223-3.

[11] N. Rockwood *et al.*, “Mycobacterium tuberculosis induction of heme oxygenase-1 expression is dependent on oxidative stress and reflects treatment outcomes,” *Front Immunol*, vol. 8, no. MAY, May 2017, doi: 10.3389/fimmu.2017.00542.

[12] A. Kumar, A. Farhana, L. Guidry, V. Saini, M. Hondalus, and A. J. C. Steyn, “Redox homeostasis in mycobacteria: the key to tuberculosis control?,” *Expert reviews in molecular medicine*, vol. 13. 2011. doi: 10.1017/s1462399411002079.

[13] M. H. Kapturczak *et al.*, “Animal Model Heme Oxygenase-1 Modulates Early Inflammatory Responses Evidence from the Heme Oxygenase-1-Deficient Mouse,” 2004.

[14] B. Wegiel *et al.*, “Carbon monoxide expedites metabolic exhaustion to inhibit tumor growth,” *Cancer Res*, vol. 73, no. 23, pp. 7009–7021, Dec. 2013, doi: 10.1158/0008-5472.CAN-13-1075.

[15] L. E. Otterbein *et al.*, “Carbon monoxide has anti-inflammatory effects involving the mitogen-activated protein kinase pathway,” *Nat Med*, vol. 6, no. 4, pp. 422–428, Apr. 2000, doi: 10.1038/74680.

[16] M. P. Soares and F. H. Bach, “Heme oxygenase-1: from biology to therapeutic potential,” *Trends Mol Med*, vol. 15, no. 2, pp. 50–58, Feb. 2009, doi: 10.1016/j.molmed.2008.12.004.

[17] Y. Naito, T. Takagi, and Y. Higashimura, “Heme oxygenase-1 and anti-inflammatory M2 macrophages,” *Archives of Biochemistry and Biophysics*, vol. 564. Academic Press Inc., pp. 83–88, Dec. 15, 2014. doi: 10.1016/j.abb.2014.09.005.

[18] S. C. Funes, M. Rios, J. Escobar-Vera, and A. M. Kalergis, “Implications of macrophage polarization in autoimmunity,” *Immunology*, vol. 154, no. 2. Blackwell Publishing Ltd, pp. 186–195, Jun. 01, 2018. doi: 10.1111/imm.12910.

[19] S. O’Leary, M. P. O’Sullivan, and J. Keane, “IL-10 blocks phagosome maturation in Mycobacterium tuberculosis-infected human macrophages,” *Am J Respir Cell Mol Biol*, vol. 45, no. 1, pp. 172–180, Jul. 2011, doi: 10.1165/rcmb.2010-0319OC.

[20] D. L. Costa *et al.*, “Pharmacological inhibition of host heme oxygenase-1 suppresses mycobacterium tuberculosis infection in vivo by a mechanism dependent on T lymphocytes,” *mBio*, vol. 7, no. 5, Sep. 2016, doi: 10.1128/mBio.01675-16.

[21] D. L. Costa *et al.*, “Heme oxygenase-1 inhibition promotes IFNγ- and NOS2-mediated control of Mycobacterium tuberculosis infection,” *Mucosal Immunol*, vol. 14, no. 1, pp. 253–266, Jan. 2021, doi: 10.1038/s41385-020-00342-x.

[22] American Academy of Pediatrics Subcommittee on Hyperbilirubinemia, “Management of hyperbilirubinemia in the newborn infant 35 or more weeks of gestation.,” *Pediatrics*, vol. 114, no. 1, pp. 297–316, Jul. 2004, doi: 10.1542/peds.114.1.297.

[23] T. D. Burt, L. Seu, J. E. Mold, A. Kappas, and J. M. McCune, “Naive Human T Cells Are Activated and Proliferate in Response to the Heme Oxygenase-1 Inhibitor Tin Mesoporphyrin,” *The Journal of Immunology*, vol. 185, no. 9, pp. 5279–5288, Nov. 2010, doi: 10.4049/jimmunol.0903127.

[24] B. W. Allwood *et al.*, “Post-tuberculosis lung health: Perspectives from the First International Symposium,” in *International Journal of Tuberculosis and Lung Disease*, International Union Against Tuberculosis and Lung Disease (The Union), Aug. 2020, pp. 820–828. doi: 10.5588/ijtld.20.0067.

[25] J. G. Pasipanodya *et al.*, “Pulmonary impairment after tuberculosis and its contribution to TB burden,” *BMC Public Health*, vol. 10, 2010, doi: 10.1186/1471-2458-10-259.

[26] K. D. Poss and S. Tonegawa, “Heme oxygenase 1 is required for mammalian iron reutilization,” 1997. [Online]. Available: www.pnas.org.
[27] J. P. Juncos *et al.*, “Anomalous renal effects of tin protoporphyrin in a murine model of sickle cell disease,” *American Journal of Pathology*, vol. 169, no. 1, pp. 21–31, 2006, doi: 10.2353/ajpath.2006.051195.
[28] C. E. Bunse *et al.*, “Modulation of heme oxygenase-1 by metalloporphyrins increases anti-viral T cell responses,” *Clin Exp Immunol*, vol. 179, no. 2, pp. 265–276, Feb. 2015, doi: 10.1111/cei.12451.
[29] J. M. Cicchese *et al.*, “Dynamic balance of pro- and anti-inflammatory signals controls disease and limits pathology,” *Immunol Rev*, vol. 285, no. 1, pp. 147–167, Sep. 2018, doi: 10.1111/imr.12671.
[30] N. V Serbina and J. L. Flynn, “Early Emergence of CD8 T Cells Primed for Production of Type 1 Cytokines in the Lungs of Mycobacterium tuberculosis-Infected Mice,” 1999.
[31] I. E. A. Flesch and S. H. E. Kaufmann, “Activation of Tuberculostatic Macrophage Functions by Gamma Interferon, Interleukin-4, and Tumor Necrosis Factor,” 1990.
[32] M. Safford *et al.*, “Egr-2 and Egr-3 are negative regulators of T cell activation,” *Nat Immunol*, vol. 6, no. 5, pp. 472–480, 2005, doi: 10.1038/ni1193.
[33] K. A. Jablonski *et al.*, “Novel markers to delineate murine M1 and M2 macrophages,” *PLoS One*, vol. 10, no. 12, Dec. 2015, doi: 10.1371/journal.pone.0145342.
[34] S. Y. Li *et al.*, “Next-Generation Diarylquinolines Improve Sterilizing Activity of Regimens with Pretomanid and the Novel Oxazolidinone TBI-223 in a Mouse Tuberculosis Model,” *Antimicrob Agents Chemother*, vol. 67, no. 4, Apr. 2023, doi: 10.1128/aac.00035-23.
[35] C. R. Scharn *et al.*, “ Heme Oxygenase-1 Regulates Inflammation and Mycobacterial Survival in Human Macrophages during Mycobacterium tuberculosis Infection ,” *The Journal of Immunology*, vol. 196, no. 11, pp. 4641–4649, Jun. 2016, doi: 10.4049/jimmunol.1500434.
[36] A. M. Cooper, “Cell-mediated immune responses in tuberculosis,” *Annual Review of Immunology*, vol. 27. pp. 393–422, 2009. doi: 10.1146/annurev.immunol.021908.132703.
[37] J. L. Flynn and J. Chan, “Immunology of tuberculosis.,” *Annu Rev Immunol*, vol. 19, pp. 93–129, 2001, doi: 10.1146/annurev.immunol.19.1.93.
[38] W. Li *et al.*, “CD38: A Significant Regulator of Macrophage Function,” *Frontiers in Oncology*, vol. 12. Frontiers Media S.A., Feb. 17, 2022. doi: 10.3389/fonc.2022.775649.
[39] F. Ahmad *et al.*, “Macrophage: A Cell With Many Faces and Functions in Tuberculosis,” *Frontiers in Immunology*, vol. 13. Frontiers Media S.A., May 06, 2022. doi: 10.3389/fimmu.2022.747799.
[40] A. Khan *et al.*, “Human M1 macrophages express unique innate immune response genes after mycobacterial infection to defend against tuberculosis,” *Commun Biol*, vol. 5, no. 1, Dec. 2022, doi: 10.1038/s42003-022-03387-9.
[41] Food and Drug Administration and GASTROINTESTINAL DRUGS ADVISORY COMMITTEE and the PEDIATRIC ADVISORY COMMITTEE, “Stannsoporfin - Proposed for the treatment of neonates greater than or equal to 35 weeks of gestational age with indicators of hemolysis who are at risk of developing severe hyperbilirubinemia,” May 2018. Accessed: Aug. 01, 2023. [Online]. Available: https://fda.report/media/112936/FDA-Briefing-Information-for-the-May-3--2018-Joint-

Meeting-of-the-Gastrointestinal-Drugs-Advisory-Committee-and-the-Pediatric-Advisory-Committee.pdf

Figures:

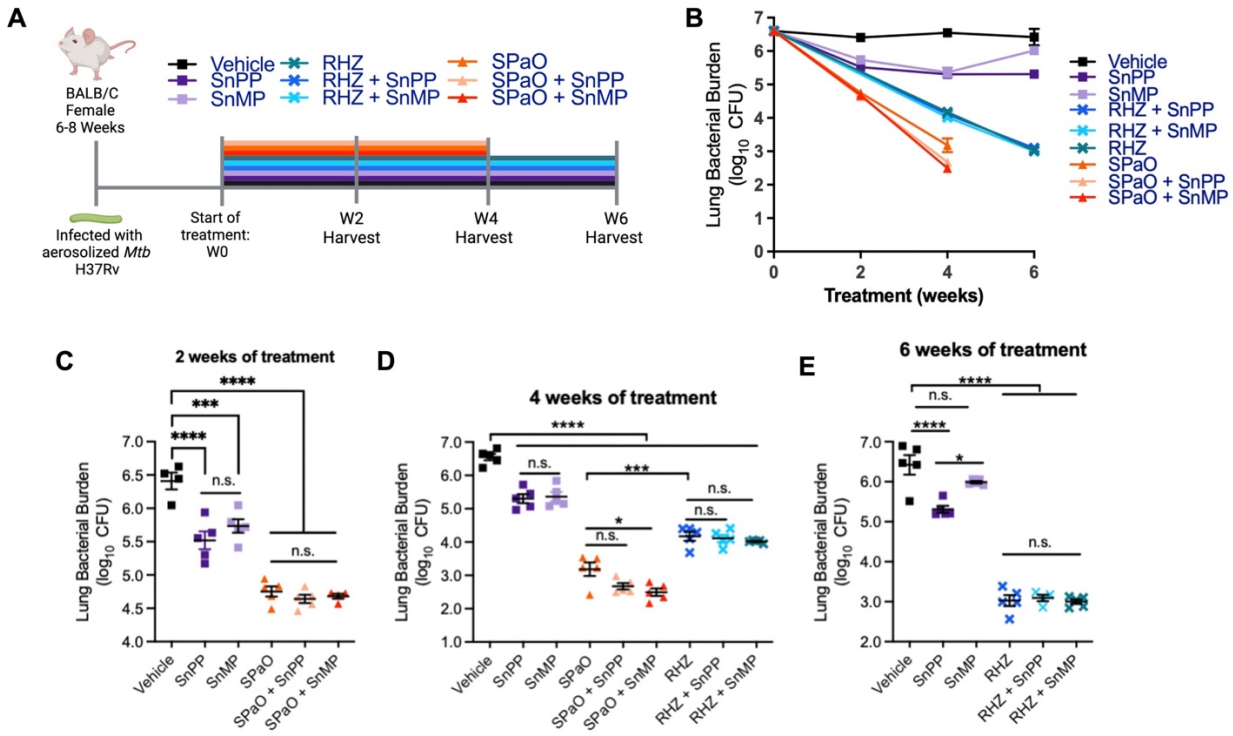

Figure 1: HO-1 inhibitors increase the antitubercular activity of a novel MDR regimen in a mouse model of chronic TB.

A) Experimental design of mouse experiments. Each line represents a different treatment group and length of treatment. BALB/c mice were aerosol-infected with ~100 bacilli of Mtb H37Rv. Treatment was initiated 4 weeks after aerosol infection. B) Mean lung bacillary burden after treatment initiation (week 0). Scatterplot of lung mycobacterial burden after 2 weeks (C), 4 weeks (D) or 6 weeks (E) of treatment. Each point represents data from individual mice. RHZ: rifampin/isoniazid/pyrazinamide; SPaO: TBAJ-876, pretomanid, TBI-223; SnPP: tin-protoporphyrin IX; SnMP: stannsoporfin; CFU: colony-forming units. *= $P < 0.05$; **= $P < 0.01$; ***= $P < 0.001$; ****= $P < 0.0001$; ns: non-statistically significant. Each experimental

group consisted of four to five mice. Statistical analysis was performed by one-way ANOVA followed by multiple comparison tests: Bonferroni and Dunnett's.

TABLE 1: Lung CFU count for time course and relapse study

	Mean lung log10 CFU count (±SD) at:				
Regimen	**dpi**	**W0**	**W2**	**W4**	**W6**
Untreated time course	3.19 ± 0.04	6.59 ± 0.10			
Vehicle			6.40 ± 0.25	6.55 ± 0.22	6.42 ± 0.54
SnPP			5.52 ± 0.29	5.30 ± 0.30	5.30 ± 0.19
SnMP			5.73 ± 0.22	5.36 ± 0.31	5.98 ±0.06
RHZ				4.17 ± 0.30	3.02 ± 0.30
RHZ + SnPP				4.11 ± 0.23	3.09 ± 0.16
RHZ + SnMP				4.01 ± 0.04	3.00 ± 0.12
SPaO			4.75 ± 0.17	3.18 ± 0.45	
SPaO + SnPP			4.64 ± 0.13	2.67 ± 0.20	
SPaO + SnMP5			4.68 ± 0.07	2.49 ± 0.25	
Untreated relapse	2.52 ± 0.10	6.18 ± 0.11			
SPaO					1.49 ± 0.27
SPaO + SnMP5					1.47 ± 0.30
SPaO + SnMP10					0.71 ± 0.23

dpi= day post infection; W0 = week 0 (start of treatment); W2 = Week 2; W4 = Week 4; W5 = Week 5; W6 = Week 6

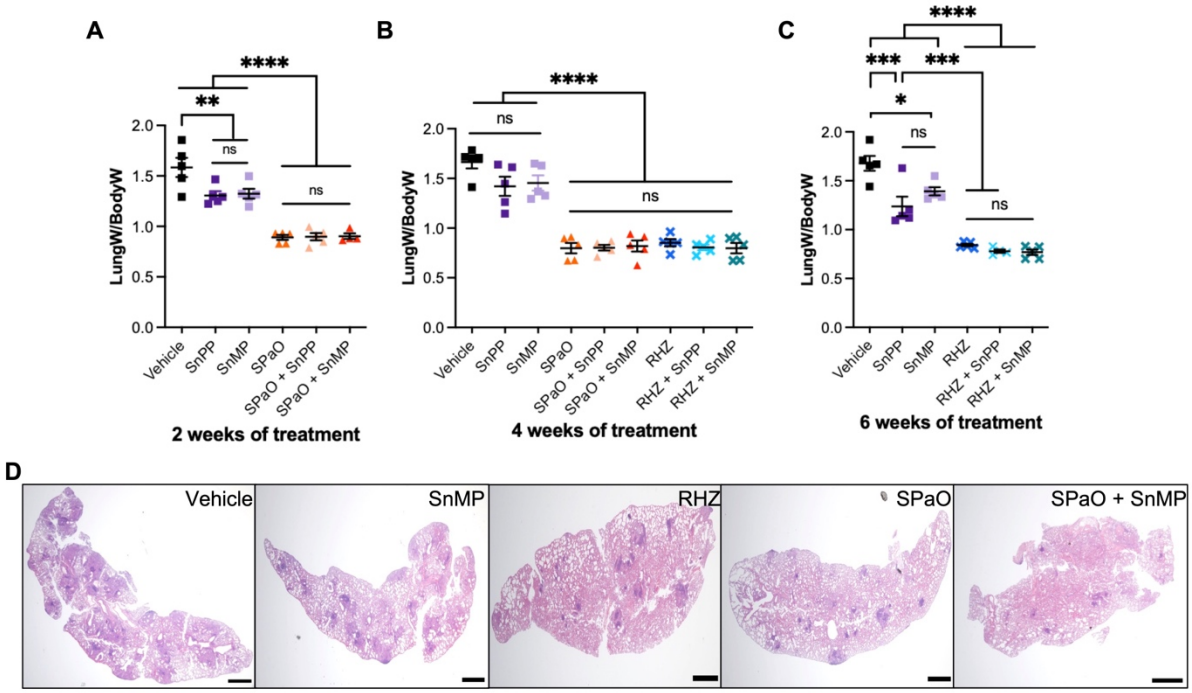

Figure 2: SnMP adjunctive therapy does not exacerbate gross lung inflammation.

A, B, C) Whole lung weight(g) to whole body weight (g) ration. Lung and body weight measurement taken at the time of harvest. D) Left lung medial apex to base were fixed with 4% paraformaldehyde and stained with H&E. Bar = 1cm. Scatterplot graphs show individual results or means ± standard deviations of the results. g: grams, RHZ:rifampin/isoniazid/pyrazinamide, SPaO: TBAJ-876 (S)/Pretomanid (Pa)/TBI-223 (O), Tin-protoporphyrin IX: SnPP, Stannsoporfin: SnMP, ns: non-statistically significant, **= $P < 0.001$; ***= $P < 0.001$, ****= $P < 0.0001$. Each experimental group consisted of four to five mice. Statistical analysis was performed by a one-way ANOVA followed by Tukeys multiple comparison test.

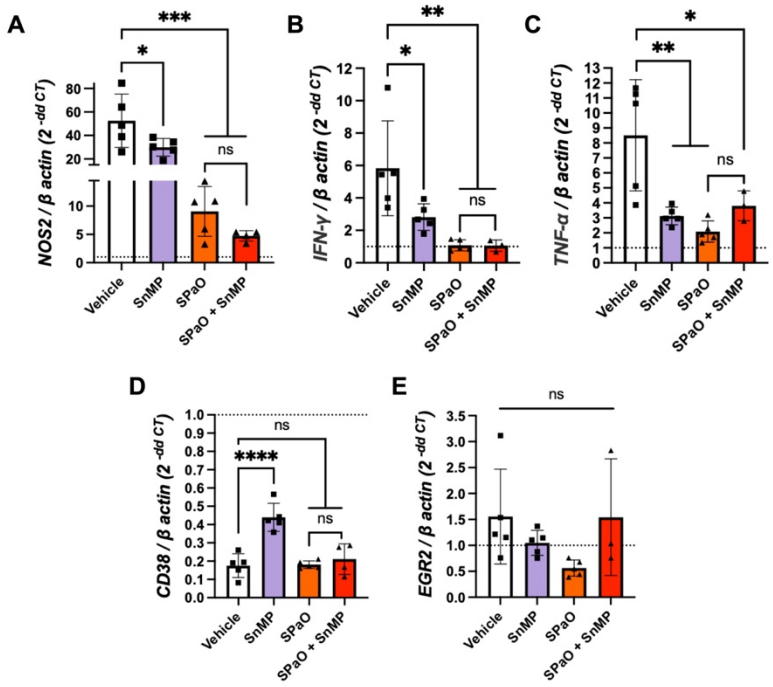

Figure 3: Genes encoding M1 macrophage markers were upregulated in the lungs after two weeks of treatment with SnMP.

RT-cPCR was performed for the expression of the following genes in snap-frozen lung homogenates: A) NOS2; B) IFN-γ; C) TNF-α; D) CD38; E) Egr2. Target gene expression was normalized relative to the housekeeping gene β-actin. The cycle number for each gene in infected test samples was normalized to that of uninfected samples. The dotted line represents the uninfected normalization of mRNA expression, SPaO: TBAJ-876 (S)/Pretomanid (Pa)/TBI-223 (O); SnMP: stannsoporfin. Data represent individual data points or means ± standard deviations of the results. ns: non-statistically significant. *= $P < 0.05$; **= $P < 0.001$; ***= $P < 0.001$, ****= $P < 0.0001$. Each bar represents a treatment group consisting of three to five mice. Statistical analysis was performed by a one-way ANOVA followed by Tukeys multiple comparison test.

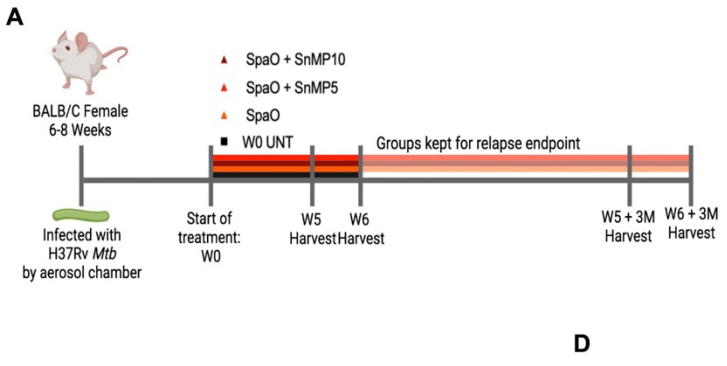

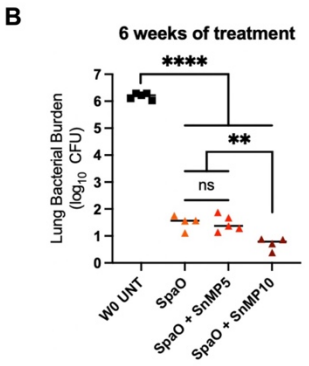

C

5 weeks + 3M group			
Treatment	**Animals Relapsed (%)**	**% Animals above 3 Log CFU**	**Log10 cfu in animals with countable CFU (SD)**
SPaO	9/9 (100)	100	
SPaO + SnMP5	20/22 (90)	80	2.5 (0.2)
SPaO + SnMP10	18/18 (100)	61	1.5 (1.1)

D

6 weeks + 3M group			
Treatment	**Animals Relapsed (%)**	**% Animals above 3 Log CFU**	**Log10 cfu in animals with countable CFU (SD)**
SPaO	6/9 (66)	66	1.9 (1.0)
SPaO + SnMP5	13/17 (76)	46	0.9 (0.8)
SPaO + SnMP10	12/18 (66)	33	1.4 (1.1)

Figure 4: Adjunctive treatment with SnMP did not help reduce relapse rates after 6 weeks of treatment, but mean lung burden upon relapse was reduced.

A) Experimental design of mouse experiments. Each line represents a different treatment group and length of treatment. B) Lung bacillary burden after 6 weeks of treatment. Each dot represents total CFU per mouse lung. C) Relapse data following treatment for a total of 5 weeks. D) Relapse data following treatment for a total of 6 weeks. W0= Week 0, W5= Week 5, W6= Week 6, WSPaO: TBAJ-876(S)/Pretomanid(Pa)/TBI-223(O), Stannsoporfin: SnMP, SnMP5: SnMP 5 mg/kg, SnMP10: SnMP 10 mg/kg. Data show individual results or means ± standard deviations of the results, **= $P < 0.001$; ****= $P < 0.0001$, ns= nonsignificant. Data in panel B represent four to five mice per treatment group. Data in panel C and D represent nine to twenty-two mice per treatment group. Statistical analysis was performed by a one-way ANOVA followed by Tukeys multiple comparison test.